The Prostate 68:92–104 (2008)

RANKL Acts Directly on RANK-Expressing Prostate Tumor Cells and Mediates Migration and Expression of Tumor Metastasis Genes

Allison P. Armstrong,[1] Robert E. Miller,[1] Jon C. Jones,[1] Jian Zhang,[2] Evan T. Keller,[2] and William C. Dougall[1]*

[1]Departments of Hematology/Oncology Research, Amgen Inc., Seattle, Washington
[2]University of Michigan, Department of Urology, School of Medicine, Ann Arbor, Michigan

BACKGROUND. Metastases to bone are a frequent complication of human prostate cancer and result in the development of osteoblastic lesions that include an underlying osteoclastic component. Previous studies in rodent models of breast and prostate cancer have established that receptor activator of NF-κB ligand (RANKL) inhibition decreases bone lesion development and tumor growth in bone. RANK is essential for osteoclast differentiation, activation, and survival via its expression on osteoclasts and their precursors. RANK expression has also been observed in some tumor cell types such as breast and colon, suggesting that RANKL may play a direct role on tumor cells.

METHODS. Male CB17 severe combined immunodeficient (SCID) mice were injected with PC3 cells intratibially and treated with either PBS or human osteprotegerin (OPG)-Fc, a RANKL antagonist. The formation of osteolytic lesions was analyzed by X-ray, and local and systemic levels of RANKL and OPG were analyzed. RANK mRNA and protein expression were assessed on multiple prostate cancer cell lines, and events downstream of RANK activation were studied in PC3 cells in vitro.

RESULTS. OPG-Fc treatment of PC3 tumor-bearing mice decreased lesion formation and tumor burden. Systemic and local levels of RANKL expression were increased in PC3 tumor bearing mice. PC3 cells responded to RANKL by activating multiple signaling pathways which resulted in significant changes in expression of genes involved in osteolysis and migration. RANK activation via RANKL resulted in increased invasion of PC3 cells through a collagen matrix.

CONCLUSION. These data demonstrate that host stromal RANKL is induced systemically and locally as a result of PC3 prostate tumor growth within the skeleton. RANK is expressed on prostate cancer cells and promotes invasion in a RANKL-dependent manner. *Prostate 68: 92–104, 2008.*

KEY WORDS: **RANK; RANKL; OPG; PC3; osteolytic lesions; prostate cancer; bone metastases**

INTRODUCTION

The majority of patients with advanced prostate cancer will develop bone metastases, and these metastases are associated with significant morbidity including pain, bone loss, fracture, hypercalcemia, and bone marrow replacement [1,2]. Prostate cancer bony metastases induce osteoblastic lesions while osteolytic

Grant sponsor: National Cancer Institute; Grant number: P01 CA093900; Grant sponsor: SPORE; Grant number: 1 P50 CA69568.

Jian Zhang's present address is Department of Medicine, University of Pittsburgh, Pittsburgh VA Healthcare System, Research and Development 151-U, University Drive, Pittsburgh, PA 15240.

*Correspondence to: William C. Dougall, Departments of Hematology/Oncology Research, Amgen Washington, 1201 Amgen Court West, Seattle, WA 98119. E-mail: dougallw@amgen.com

Received 17 June 2007; Accepted 18 September 2007
DOI 10.1002/pros.20678
Published online 15 November 2007 in Wiley InterScience (www.interscience.wiley.com).

lesions are typically observed with multiple myeloma and breast cancer. The osteoblastic or osteolytic character of bone metastases actually represents two extremes of a spectrum in which dysregulation of the normal bone remodeling process occurs [2–5]. The notion that total bone remodeling [6] is increased in patients with prostate cancer bone metastases is supported by histological evidence of osteoclast action [7] and the increases in markers of bone resorption (e.g., *N*-telopeptide of type I collagen, or NTX) [8]. The mechanisms by which tumor cells co-opt the normal processes of bone remodeling and the reciprocal feedback of the bone microenvironment to the bone are central to the pathophysiology of metastatic bone disease.

The RANK/RANKL/OPG axis governs osteoclastogenesis and bone resorption [9]. The TNF ligand superfamily member RANKL is critical for formation, function, and survival of osteoclasts [10,11] and exerts its action through binding and activation of its receptor RANK [12,13], which is expressed on the surface of myeloid osteoclast precursors [14]. Osteprotegerin (OPG) is a soluble member of the TNF receptor super family secreted by osteoblasts which, by competing with RANK for RANKL, acts as a decoy receptor of RANKL, thereby inhibiting osteoclastogenesis. The stimulation of osteoclastogenesis observed in bone metastases is frequently a result of increases in RANKL and/or decreases in OPG levels [15]. The complete block of tumor-induced osteolytic lesions by RANKL inhibitors (e.g., RANK-Fc or OPG-Fc) in animal models of bone metastases demonstrates the vital role of this factor in cancer-induced bone disease [16,17], including that mediated by prostate cancer [18].

In addition to the expression of RANK on hematopoietic osteoclast precursors, this receptor has also been observed in some tumor cell types [19,20] and RANKL may therefore play a role in the migration and metastatic behavior of cancer in the skeleton. In this study we analyzed the expression of RANK mRNA and protein on prostate cancer cells and demonstrated that activation of RANK by RANKL results in multiple downstream signaling events and changes in global gene expression which may ultimately affect tumor metastasis.

MATERIALS AND METHODS

Tumor Cell Lines

PC3, LNCaP, DU145, MDAPCa2b, and 22Rv1 prostate cancer lines were obtained from ATCC. PC3, LNCaP, 22Rv1, and DU145 cells were cultured in RPMI with 10% fetal bovine serum (FBS). MDAPCa2b were grown in BRFF HPCI with 20% FBS (Athena Enzyme Systems, Baltimore, MD). C42B cells were obtained from UroCor, Inc. (Oklahoma City, OK) and grown in T-media [21].

PC3 Xenograft Experiments

At 8 weeks of age, male CB17 severe combined immunodeficient (SCID) mice (Charles River Laboratories, Wilmington, MA) were injected with 1×10^5 PC3 cells intratibially. Mice were treated with either PBS or 3 mg/kg human OPG-Fc (Amgen, Inc., Thousand Oaks, CA) 3× weekly subcutaneously beginning either 7 or 20 days after inoculation. The presence of osteolytic lesions was assessed by digital X-ray (Faxitron, Wheeling, IL). Tumors were allowed to progress until day 24 or 27 at which time mice were sacrificed. Lesion area was calculated from digital images using MetaMorph® Imaging software (Molecular Devices Corporation, Downingtown, PA).

Histopathology

Femurs and tibias were harvested and fixed in 10% neutral-buffered formalin. Bones were decalcified in 10% formic acid for 4 days and embedded in paraffin. Formalin-fixed paraffin-embedded sections were cut at 0.4 μm and stained with hematoxylin and eosin. Tumor burden was quantified on hematoxylin stained sections using MetaMorph® Imaging software (Molecular Devices Corporation). Additional sections were stained for tartrate-resistant acid phosphatase (TRAP) activity (Sigma-Aldrich, St. Louis, MO). Murine RANK and murine RANKL expression were detected using antibodies AF692 and AF462, respectively, from R&D Systems (Minneapolis, MN).

mRNA Expression Analysis

Total RNA was isolated from tumor cell lines or mouse tibias using the RNAeasy™ Kit (Qiagen, Valencia, CA) and transcribed into cDNA using random hexamer priming and TaqMan™ Reverse Transcription Reagents (Applied Biosystems, Inc., Foster City, CA). Tumor cell or tibia cDNA (10 ng or 25 ng, respectively) was analyzed for gene of interest expression using Assay on Demand™ primer probe sets (Applied Biosystems, Inc.). Quantitative real-time reverse transcriptase polymerase chain reaction (RT-PCR) was performed using the ABI Prism 7900HT Sequence Detection System (Applied Biosystems, Inc.). Gene expression was calculated relative to β-actin expression. Reactions were performed in triplicate.

Human RANK Protein Expression

Surface RANK expression was determined by flow cytometry after incubation with either 1 μg/ml mouse

anti-RANK antibody (Amgen) or isotype control (BD Biosciences, San Jose, CA) in 2% FBS followed by allophycocyanin (APC)-conjugated anti-mouse secondary antibody. Fluorescence was assessed using a FAScan sorter (BD Biosciences).

Immunoblot Analysis and Nuclear Translocation Assays

PC3 cells were grown in serum-free RPMI overnight prior to stimulation with 1 μg/ml recombinant human RANKL (Amgen) for the times indicated. For immunoblot analysis, cells were stimulated with RANKL and harvested in 1× cell lysis buffer (Cell Signaling, Danvers, MA) supplemented with 1 mM phenylmethylsulfonyl fluoride and 1 mM sodium fluoride. The soluble fraction of whole-cell lysate (15 μg) was separated on 8–16% Tris–Glycine gels and electroblotted onto nitrocellulose membranes. Membranes were blocked in 5% non-fat dry milk and subsequently incubated with antibodies to phosphorylated or total ERK, JNK, or MAP kinase p38 (Cell Signaling) at 1:1,000 overnight at 4°C. Blots were incubated in anti-rabbit horseradish peroxidase (HRP; Santa Cruz Biotechnology, Santa Cruz, CA) at 1:2,000, washed, and developed using electrochemilumincent (ECL) imaging (GE Healthcare, Buckinghamshire, UK). To measure nuclear translocation of phosphorylated forms of p38, c-Jun, or ATF-2, cells were grown overnight in serum-free RPMI and stimulated with 1 μg/ml RANKL (Amgen) for the times indicated. Indirect immuofluorescence reagents from ''Hit Kits'' (Cellomics, Inc., Pittsburgh, PA) were used for cell staining. Nuclear and cytoplasmic expression was quantified using software from Cellomics, Inc.

Gene Expression Analysis

Cells were grown in RPMI containing 10% FBS and stimulated with 1 μg/ml human recombinant RANKL (Amgen). mRNA was isolated with the RNAeasy Kit (Qiagen). For microarray expression analysis, 5 μg of total mRNA was labeled using standard protocols (Affymetrix, Santa Clara, CA) and 10 μg biotinylated cRNA was hybridized to Human Affymetrix U133A chip consisting of approximately 22,000 probe sets representing 14,500 genes. Hybridized chips were stained and washed on an Affymetrix FS400 fluidics station using the antibody amplification protocol and scanned using an Affymetrix GeneArray 2500 scanner. Scanned images were loaded into the Resolver™ system (Rosetta Biosoftware, Seattle, WA) for analysis.

Cytokine Analysis

Cells were grown in RPMI containing 10% FBS and stimulated with 1 μg/ml human recombinant RANKL (Amgen). Supernatant was harvested after 48 hr. Cytokine levels were measured using ELISAs from R&D Systems and or the Human Cytokine/Chemokine panel from LinCo (Billerica, MA).

Cell Invasion Assay

Recombinant human RANKL and recombinant human OPG were obtained from PeproTech, Inc. (Rocky Hill, NJ). The cell invasion assay was performed as described previously [22]. Briefly, 2.5×10^4 PC3 cells in 0.5 ml RPMI-1640 medium containing 1% FBS were seeded into the upper compartment of two-layer chamber invasion plates that were separated by an uncoated membrane (for baseline control) or a membrane coated with collagen matrix (BD Transduction Laboratory, Bedford, MA). The cells were cultured for 48 hr followed by staining of the membrane with a Diff-Quik stain kit (Dade Behring, Inc, Newark, DE). Cells were quantified by counting the numbers of cells that penetrated the membrane in five microscopic fields (at 200× magnification) per filter. Invasive ability was defined as the proportion of cells that invaded the matrix-coated membrane divided by the number of cells that migrated through the uncoated membrane (baseline migration). The results are reported as the mean of duplicate assays.

Statistical Analysis

Statistical analysis of data was performed using Prism Software (GraphPad Software, San Diego, CA). For comparison of two groups, Student's *t*-test was used. Welch's correction of variance was used when necessary. For data comparisons with three or more groups, one-way analysis of variance (ANOVA) with Tukey's post-test was used.

RESULTS

PC3 Prostate Cancer Cells Induce Osteolysis Via Increases in RANKL

It is well established that the prostate cancer cell line PC3 promotes osteolysis in murine experimental metastases models [23,24]. We hypothesized that PC3 cells may alter RANKL and/or OPG levels, subsequently leading to increased osteoclastogenesis. We verified the extent of PC3-induced osteolytic lesions by radiographic and histologic analysis following intratibial inoculation of PC3 cells into CB17 SCID mice (Fig. 1A,B). Osteolysis was evident by radiographic analysis at 14 days post-inoculation (Fig. 1A). The progression of these lesions over time was significant (Fig. 1A; $P < 0.01$ for day 24 vs. day 7 and $P < 0.05$ for day 24 vs. day 14). Osteolysis was associated with tumor burden and increased numbers of osteoclasts at the

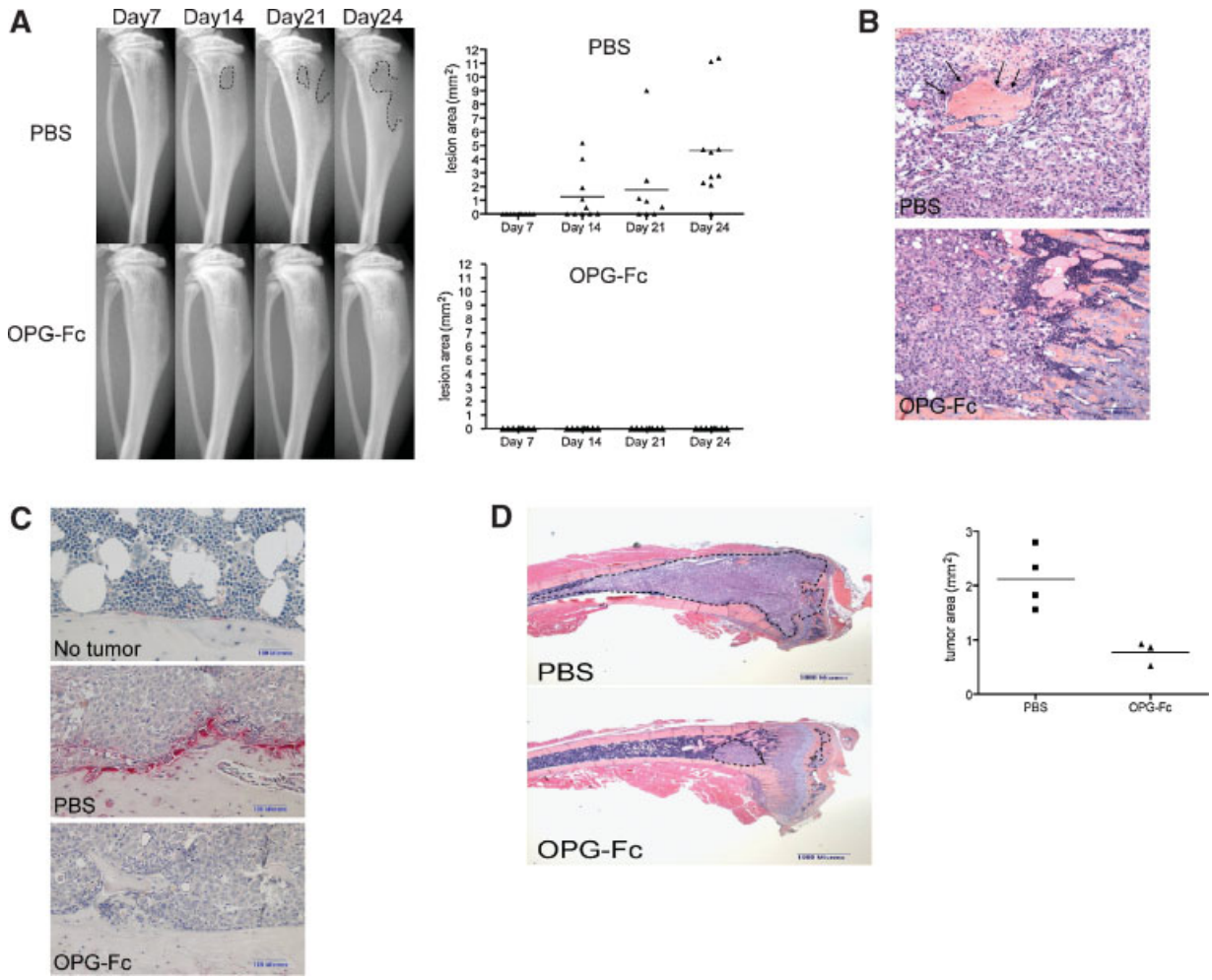

Fig. 1. OPG-Fc treatment of PC3 tumor bearing mice reduced osteolytic lesion formation, osteoclast numbers, and tumor burden. **A**: OPG-Fc treatment inhibited progression of PC3 cell induced osteolytic lesions relative to PBS treated mice. CBI7 SCID mice were injected with 1×10^5 PC3 cells intratibially. Mice were treated with either PBS or 3 mg/kg human OPG-Fc subcutaneously 3× weekly beginning at day 7. X-rays were taken at days 7, 14, 21, and 24 post-injection. Osteolytic regions are outlined. Quantification of lesions revealed progression over time in PBS-treated mice was significant; $P < 0.01$ for day 24 versus day 7 and $P < 0.05$ for day 24 versus day 14. **B**: Osteolysis is reduced in OPG-Fc treated mice histologically. Paraffin embedded sections were stained with hematoxylin and eosin. Arrows indicated areas of osteolysis in PBS treated bone. **C**: OPG-Fc treatment reduced the number of TRAP positive osteoclasts in bone. Paraffin embedded sections were stained for TRAP activity (red) and counterstained with hematoxylin. **D**: PC3 intratibial tumor burden was decreased in OPG-Fc treated mice. CBI7 SCID mice were injected with 1×10^5 PC3 cells intratibially. Mice were treated with either PBS or 3 mg/kg human OPG-Fc subcutaneously 3× weekly beginning at day 20 and sacrificed on day 27. Paraffin embedded sections were stained with hematoxylin and eosin. Tumor area is outlined by dashed line. Quantification of sections demonstrated a significant decrease in tumor burden in OPG-Fc treated mice, $P = 0.01$.

tumor/bone interface compared with naïve mice (Fig. 1B,C). Osteoclasts were also observed within the tumor mass (data not shown).

To determine the relative contribution of murine host stromal RANKL versus human PC3 tumor cell RANKL expressed at tumor sites, we analyzed RANKL mRNA expression using mouse- and human-specific RT-PCR primers. There was a significant increase in mouse RANKL expression in tibias with tumor compared with contralateral non-tumor-bearing tibias at day 21 post-injection (Fig. 2A, $P < 0.01$). Human RANKL mRNA was expressed at low levels in PC3 cells in vitro, but was not detectable in tumor-bearing tibias of mice at day 21 (data not shown). Murine OPG mRNA was also significantly increased in tumor-bearing tibias (Fig. 2A, $P < 0.05$). However, the increase in endogenous OPG was clearly not sufficient to block RANKL, as indicated by the dramatic increase in the tumor-induced osteoclastogenesis that was observed (Fig. 1C; naïve vs. PBS). Murine RANK mRNA levels were increased approximately twofold ($P = 0.06$) in tumor-bearing tibias as compared with

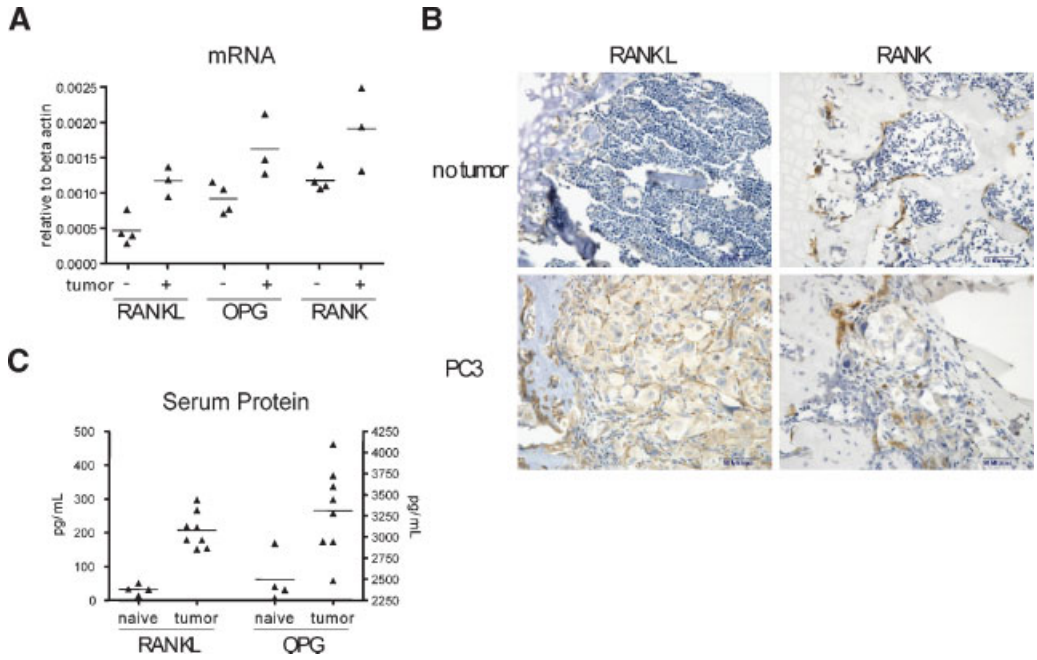

Fig. 2. PC3 tumor growth in vivo resulted in increases in local and systemic RANKL. **A**: Murine RANKL and OPG mRNA expression were increased in tumor-bearing tibias. RNA was isolated from tumor-bearing and non-tumor-bearing tibias 21 days after PC3 cell injection. Murine RANKL, OPG, and RANK expression was determined by quantitative real-time RT-PCR and is shown relative to β-actin from the same sample; $P < 0.01$ for RANKL tumor- versus non-tumor-bearing tibia, $P < 0.05$ for OPG, $P = 0.06$ for RANK. **B**: Murine RANKL protein expression was increased in the stroma of PC3 tumor bearing mice. Paraffin embedded sections were stained for RANKL or RANK (in brown) and counter-stained with hematoxylin. **C**: Serum murine RANKL and OPG levels were increased in PC3-tumor bearing mice. Serum levels of RANKL and OPG in PC3 tumor-bearing mice and age-matched naïve controls were measured by ELISA; $P < 0.0001$ for RANKL naïve versus tumor-bearing mice, $P < 0.05$ for OPG.

controls, presumably reflecting the increases in OCL numbers observed (Fig. 2A). We observed similar increases in murine RANKL and RANK protein in histological sections of naïve and tumor bearing bone (Fig. 2B). In naïve mice, low levels of murine RANKL expression were detected using immunohistochemistry in stromal cells and preosteoblasts. Tumor bearing mice demonstrated an increase in RANKL positive stromal cells located at the tumor/bone interface and within the tumor (Fig. 2B). Using IHC and antibodies against RANK, a small increase in the number of RANK positive cells, specifically mature osteoclasts and osteoclast precursors, was observed in tumor bearing mice.

We also determined the effect of PC3 tumor cell growth in vivo on systemic levels of murine RANKL and OPG. Serum murine RANKL in PC3 tumor-bearing mice was increased approximately sixfold over that of naïve mice (Fig. 2C, $P < 0.0001$). Serum murine OPG levels were increased less than twofold (Fig. 2C, $P < 0.05$). Although PC3 cells secrete OPG in vitro, human OPG was undetectable in the serum (data not shown). These alterations in murine RANKL and OPG levels resulted in a fivefold increase in the RANKL/OPG molar ratio in serum of tumor-bearing versus control animals (data not shown, $P < 0.01$).

To test the hypothesis that RANKL is a critical mediator of the tumor-induced osteoclastogenesis, we evaluated the ability of a RANKL inhibitor, recombinant human OPG-Fc, to block the progression of osteolytic lesions in bone. In contrast to the increase in skeletal lesions observed in PBS treated, tumor-bearing animals, mice that were treated with OPG-Fc (3 mg/kg, 3 times/week) beginning at day 7 showed no evidence of osteolytic lesions (Fig. 1A,B). Treatment with OPG-Fc eliminated tumor-induced osteoclasts (Fig. 1C) and significantly decreased tumor burden (Fig. 1D, $P = 0.01$). These data support a model in which tumor-associated factors converge on the mouse stroma to cause local increases in RANKL, in turn leading to the dramatic increases in osteoclasts.

RANK Is Expressed on Prostate Cancer Cell Lines

Our results indicate a role for the tumor-induced stromal RANKL in osteolytic lesion development after PC3 tumor establishment in the skeleton. The functional role of RANK on mammary epithelial cells [25] and tumors of epithelial origin [19,26,20] suggests

that stromal RANKL could also contribute to skeletal metastasis via direct activation of RANK expressed by tumor cells. We examined several prostate cancer cell lines established from primary tumor (22Rv1) or metastases to lymph node (LNCaP), brain (DU145), or bone (PC3, MDAPCa2b, C42B) for RANK expression. These six lines represent androgen-dependent (LNCaP, 22Rv1, and MDAPCa2b) and androgen-insensitive (PC3, DU145, C42B) prostate cancers [27,28]. RANK mRNA was detected by quantitative real-time RT-PCR in LNCaP, DU145, C42B, and PC3 cells (Fig. 3A). We did not observe RANK mRNA expression in 22Rv1 and MDAPCa2b cell lines (data not shown). Since a functional response to RANKL requires expression of RANK on the cell surface we used flow cytometry to examine these prostate lines for RANK. LNCaP, DU145, C42B, and PC3 cells all expressed RANK on the cell surface, with PC3 cells showing particularly high levels (Fig. 3B). These data demonstrate RANK expression in prostate cancer cell lines derived from a variety of stages of disease.

RANKL Induces Multiple Signaling Pathways in PC3 Cells

RANK activation has been shown to lead to downstream signaling events including mitogen-activated protein (MAP) kinase p38, extracellular signal-regulated kinase (ERK), c-Jun NH_2 kinase (JNK), and NF-κB pathways [20,29–31]. Treatment of PC3 cells with RANKL resulted in rapid (within 5 min) stimulation of MAP kinase p38 and ERK phosphorylation (Fig. 4A). RANKL-dependent JNK phosphorylation occurred 15 min after treatment (Fig. 4A). We expanded upon these findings by investigating the ability of RANKL to induce signaling events downstream of MAP kinase p38 and JNK. Within 15 min of RANKL exposure, phosphorylated forms of MAP kinase p38, c-Jun, and ATF-2 translocated to the nucleus (Fig. 4B), confirming the activation of MAP kinase p38 and JNK signaling pathways by RANKL.

RANK Signaling Results in Changes in Global Gene Expression in PC3 Cells

To further characterize the consequences of RANK activation in PC3 cells, we performed gene expression analysis using the Affymetrix U133A chip on PC3 cells treated with 1 μg/ml RANKL for 6, 12, or 24 hr. We identified genes that were regulated by RANKL activation of RANK at each timepoint, with the greatest number and magnitude of changes in expression observed at 24 hr (Table I and data not shown). Analysis of bioduplicate samples of control and RANKL-treated cells at 24 hr resulted in identification of 52 probe sets (representing 42 genes) regulated greater than twofold with $P < 0.05$. The expression of 35 probe sets (representing 28 genes) was increased in the presence of RANKL while 17 probe sets representing 14 genes reflected a decrease in expression.

We chose to focus on genes that had previously been identified as either regulated by RANKL in other cell systems (e.g., osteoclasts), increased in disease-associated osteolysis, or capable of stimulating cell migration. We looked at genes upregulated in response to RANKL during osteoclastogenesis (identified in Chaisson et al. [6]), and studied the regulation of a subset of these genes in PC3 cells. Using RT-PCR we confirmed that MMP-9 was upregulated approximately 25-fold in PC3 cells at 12 hr post-RANKL stimulation (Fig. 5A). Amongst the factors which have been implicated in stimulation of osteoclasts and involvement in osteolysis in disease states (reviewed in Ref. [15]), we observed the upregulation of CSF-1, IL-1β, TNF-α, IL-8, and IL-6 by array analysis and confirmed these gene expression changes by RT-PCR. The greatest fold induction of IL-6 was 30-fold at 12 hr, whereas maximal induction of CSF-1, IL-1β, TNF-α,

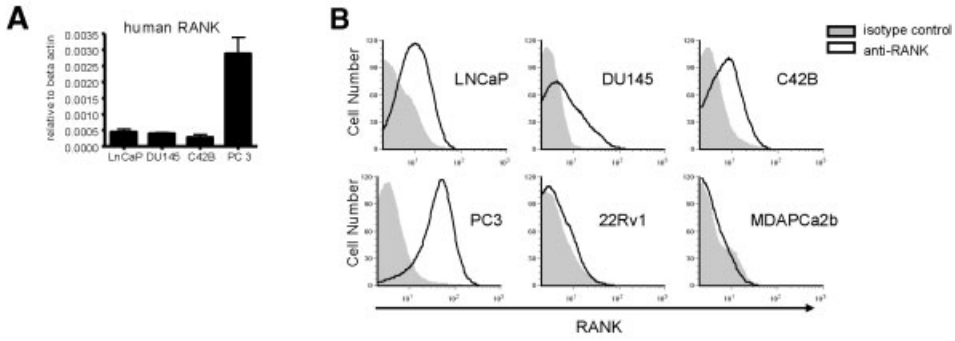

Fig. 3. RANK mRNA and protein was expressed in human prostate cancer cell lines. **A**: RANK mRNA was detected in prostate cancer lines. cDNA (10 ng) was subjected to quantitative real-time RT-PCR. RANK expression is shown relative to β-actin of the same sample. **B**: RANK protein was expressed on the surface of prostate cancer cell lines. Cells were stained with RANK-specific antibody or isotype control and APC-conjugated secondary antibody, and RANK expression was assessed by flow cytometry.

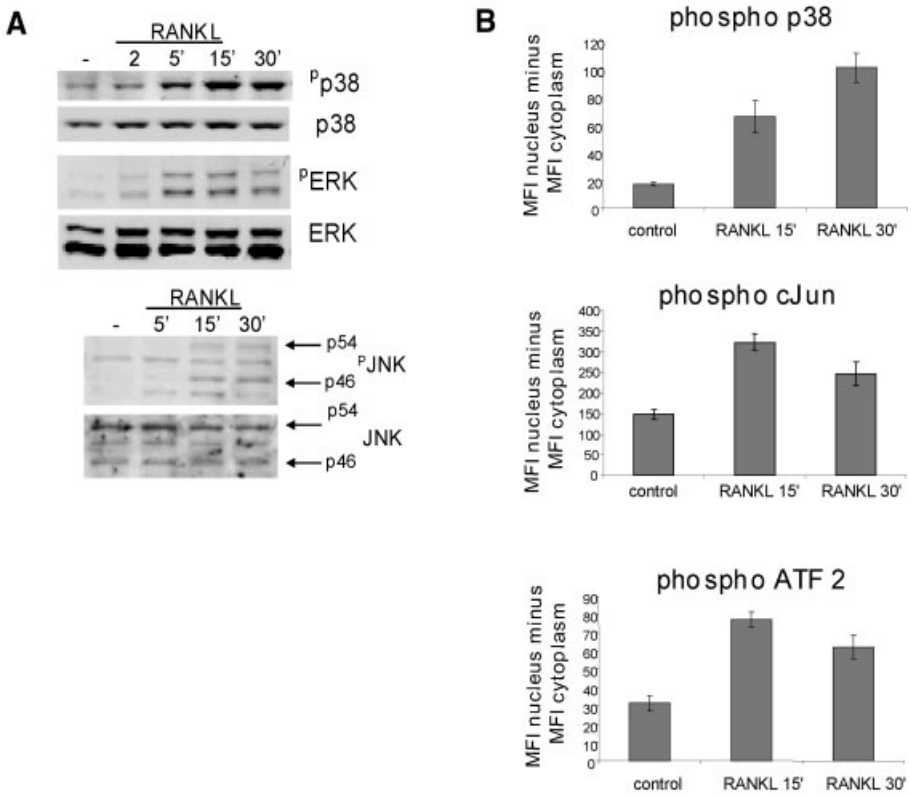

Fig. 4. RANKL mediated activation of multiple signaling pathways in PC3 cells. **A**: RANK activation resulted in phosphorylation of MAP kinase p38, ERK, and JNK. PC3 cells were stimulated with 1 μg/ml RANKL for the times indicated. Whole cell lysate (15 μg) was used for immunoblot analysis of the indicated proteins. **B**: RANK activation resulted in translocation of the phosphorylated forms of p38, c-Jun, and ATF-2 to the nucleus. Cells were stimulated with 1 μg/ml RANKL for the times indicated, then fixed and immunostained for the phosphorylated forms of p38, c-Jun, or ATF-2. Cellomics software was used to determine the difference between the mean fluorescence intensity (MFI) of the nucleus versus the MFI of the cytoplasm.

and IL-8 was approximately three- to fourfold at 24 hr after RANKL treatment (Fig. 5A). Array analysis revealed upregulation of CXCL-1, CXCL-2, CXCL-3, CXCL-5, CXCL-6, and IL-8, members of the C-X-C chemokine family which can stimulate migration and chemotaxis of tumor and immune cells [32,33]. Using RT-PCR analysis, we confirmed that CXCL-1, CXCL-2, CXCL-3, CXCL-5, CXCL-6, and IL-8 were upregulated 3- to 12-fold in PC3 cells stimulated for 24 hr with RANKL (Fig. 5A).

We expanded upon the observed gene expression changes by confirming the regulation of protein levels using cytokine specific ELISAs. Analysis of the conditioned media of PC3 cells 24 hr post-stimulation with RANKL demonstrated that CXCL-1, CXCL-5, CXCL-6, IL-6, and IL-8 protein levels were increased three- to fourfold (Fig. 5B). We expanded on these findings by using a multiplex ELISA to analyze the levels of 29 different cytokines in PC3 conditioned media after RANKL treatment. We identified two additional proteins, GM-CSF and VEGF-A, in the cytokine panel that were increased in response to RANKL but had not been previously identified by array analysis (Fig. 5B). These observed RANKL-dependent protein changes were abrogated by the addition of OPG-Fc (data not shown). Upregulation of these cytokines was also stimulated by an agonistic antibody to RANK (data not shown). Together these data support the idea that RANKL-induced changes on PC3 cells were specifically via stimulation of RANK on the tumor cells.

RANKL Stimulates Invasion of PC3 Cells Through Collagen

Previous work has shown that RANKL increases the survival of osteoclasts [11] and is important for the proliferation and survival of mammary epithelial cells during pregnancy [25]. To investigate the pro-metastatic effects of RANK stimulation on prostate cancer cells, we studied the effect of RANKL treatment on PC3 cell proliferation, viability, and cell invasion. Under a variety of conditions, RANKL did not detectably alter PC3 cell proliferation in vitro (data not shown). Additionally, RANKL treatment did not affect the sensitivity of PC3 cells to a variety of

TABLE I. Genes Differentially Regulated in Response to RANKL

Accession id	Probe set	Gene name	Gene description	Fold change	*P*-value
NM_002994	215101_s_at	CXCL5	Chemokine (C-X-C motif) ligand 5	18.19	1.86E-10
NM_017870	218834_s_at	TMEM132A	Transmembrane protein 132A	15.30	0.00145
NM_003900	213112_s_at	SQSTM1	Sequestosome 1	14.76	0.00164
NM_001165	210538_s_at	BIRC3	Baculoviral IAP repeat-containing 3	10.14	7.88E-15
NM_002994	214974_x_at	CXCL5	Chemokine (C-X-C motif) ligand 5	8.69	3.49E-14
NM_000584	211506_s_at	IL8	Interleukin 8	7.63	4.35E-07
NM_006850	206569_at	IL24	Interleukin 24	7.33	0.00058
NM_015541	211596_s_at	LRIG1	Leucine-rich repeats and immunoglobulin-like domains 1	6.50	0.00035
NM_004666	205844_at	VNN1	Vanin 1	5.34	0.00085
NM_016584	220054_at	IL23A	Interleukin 23, alpha subunit p19	4.82	1.36E-19
NM_016235	203632_s_at	GPRC5B	G protein-coupled receptor, family C, group 5, member B	4.45	8.91E-07
NM_002089	209774_x_at	CXCL2	Chemokine (C-X-C motif) ligand 2	4.17	1.15E-09
NM_020529	201502_s_at	NFKBIA	Nuclear factor of kappa light polypeptide gene enhancer in B-cells inhibitor, alpha	3.96	7.87E-21
NM_002638	203691_at	PI3	Peptidase inhibitor 3, skin-derived (SKALP)	3.39	2.67E-07
NM_002090	207850_at	CXCL3	Chemokine (C-X-C motif) ligand 3	3.15	0.00335
NM_001077493	207535_s_at	NFKB2	Nuclear factor of kappa light polypeptide gene enhancer in B-cells 2	3.02	5.16E-07
NM_002192	204926_at	INHBA	Inhibin, beta A (activin A, activin AB alpha polypeptide)	2.90	1.70E-06
NM_000043	215719_x_at	FAS	Fas (TNF receptor superfamily, member 6)	2.85	0.00153
NM_000584	202859_x_at	IL8	Interleukin 8	2.81	1.05E-18
NM_006290	202644_s_at	TNFAIP3	Tumor necrosis factor, alpha-induced protein 3	2.75	1.00E-10
NM_002993	206336_at	CXCL6	Chemokine (C-X-C motif) ligand 6	2.67	9.88E-17
NM_014903	204823_at	NAV3	Neuron navigator 3	2.52	0.00317
NM_000576	205067_at	IL-1β	Interleukin 1, beta	2.37	7.72E-22
NM_006058	207196_s_at	TNIP1	TNFAIP3 interacting protein 1	2.34	6.95E-12
NM_001511	204470_at	CXCL1	Chemokine (C-X-C motif) ligand 1	2.31	3.18E-19
NM_005257	210002_at	GATA6	GATA binding protein 6	2.30	6.80E-09
NM_001945	38037_at	HBEGF	Heparin-binding EGF-like growth factor	2.22	0.00152
NM_000593	202307_s_at	TAP1	Transporter 1, ATP-binding cassette, sub-family B (MDR/TAP)	2.22	0.00228
NM_001109	205180_s_at	ADAM8	ADAM metallopeptidase domain 8	2.19	0.00004
NM_006290	202643_s_at	TNFAIP3	Tumor necrosis factor, alpha-induced protein 3	2.19	0.00064
NM_000576	39402_at	IL-1β	Interleukin 1, beta	2.15	5.78E-21
NM_002638	41469_at	PI3	Peptidase inhibitor 3, skin-derived (SKALP)	2.15	7.90E-08
NM_003900	201471_s_at	SQSTM1	Sequestosome 1	2.14	2.53E-11
NM_002192	210511_s_at	INHBA	Inhibin, beta A (activin A, activin AB alpha polypeptide)	2.02	4.31E-10
NM_006509	205205_at	RELB	v-rel reticuloendotheliosis viral oncogene homolog B, (avian)	2.01	0.00255
NM_003713	212226_s_at	PPAP2B	Phosphatidic acid phosphatase type 2B	−2.02	1.49E-09
NM_003286	208900_s_at	TOP1	Topoisomerase (DNA) I	−2.02	2.94E-09
NM_003607	214464_at	CDC42BPA	CDC42 binding protein kinase alpha (DMPK-like)	−2.02	9.00E-07
NM_001006946	201286_at	SDC1	Syndecan 1	−2.06	1.02E-14
NM_005242	206429_at	F2RL1	Coagulation factor II (thrombin) receptor-like 1	−2.06	3.02E-06
NM_001394	204015_s_at	DUSP4	Dual specificity phosphatase 4	−2.08	7.55E-08
NM_002275	204734_at	KRT15	Keratin 15	−2.11	0.00415
NM_018897	214222_at	DNAH7	Dynein, axonemal, heavy chain 7	−2.16	0.00056
NM_003713	209355_s_at	PPAP2B	Phosphatidic acid phosphatase type 2B	−2.30	1.70E-06
NM_001394	204014_at	DUSP4	Dual specificity phosphatase 4	−2.42	1.31E-17
NM_000860	211548_s_at	HPGD	Hydroxyprostaglandin dehydrogenase 15-(NAD)	−2.67	7.57E-07
NM_001040708	218839_at	HEY1	Hairy/enhancer-of-split related with YRPW motif 1	−2.68	3.56E-12
NM_000489	208859_s_at	ATRX	RAD54 homolog, *S. cerevisiae*	−2.68	5.86E-06
XM_001128030	213605_s_at	LOC728411	Similar to Beta-glucuronidase precursor	−2.89	0.00496
NM_000599	211959_at	IGFBP5	Insulin-like growth factor binding protein 5	−3.02	1.03E-19
NM_006408	209173_at	AGR2	Anterior gradient 2 homolog (*Xenopus laevis*)	−3.16	6.76E-07
NM_000599	203424_s_at	IGFBP5	Insulin-like growth factor binding protein 5	−6.10	9.39E-08

Genes regulated by RANKL with greater than twofold expression differences relative to untreated cells and their associated *P*-values are shown. Affymetrix probe set identifiers, gene descriptions, and gene accession numbers are included.

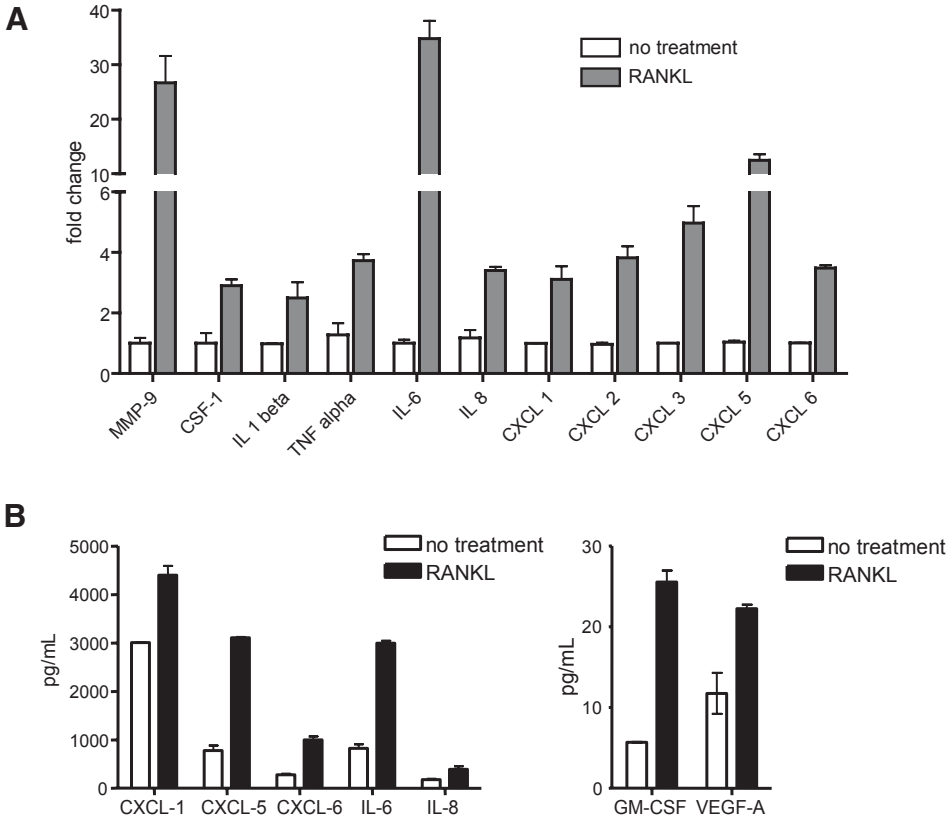

Fig. 5. RANKL induced changes in gene expression were confirmed at the mRNA and protein levels. **A**: mRNA levels of genes identified by array were increased in response to RANKL. mRNA was isolated from PC3 cells 12 hr (MMP-9, IL-6) or 24 hr (all other genes) after RANKL treatment. Gene expression was determined by quantitative real-time RT-PCR, normalized to β-actin and expressed relative to untreated cells. **B**: Protein levels of genes identified by array were increased in response to RANKL. Supernatant was collected 48 hr after RANKL treatment and cytokine levels determined by ELISA.

chemotherapeutics, including, CPT-11, doxorubicin, 5-Florouracil, etoposide, or cisplatin (data not shown).

RANKL has been shown to stimulate chemotaxis of osteoclast-like cells and RANK-expressing tumor cells [19,34,35]. Given that RANKL is expressed in the bone microenvironment and PC3 tumor cells express RANK, we hypothesized that RANKL might serve as a ''soil'' factor that stimulates migration of PC3 cells to bone. We studied the effect of RANKL on invasion of PC3 cells through a collagen matrix and found that invasion was increased significantly in the presence of RANKL (Fig. 6, $P < 0.05$ RANKL treated versus

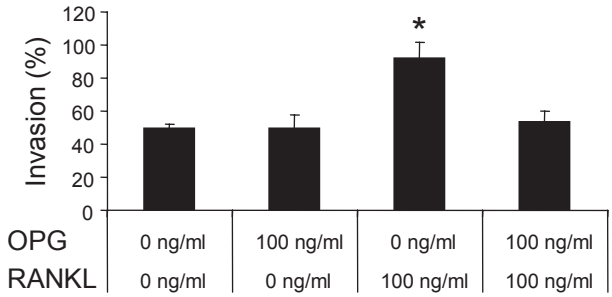

Fig. 6. RANKL stimulated migration of PC3 cells through collagen matrix. PC3 cells were seeded into the upper compartment of two-layer chamber invasion plates that were separated by an uncoated membrane (for baseline control) or a membrane coated with collagen matrix. The cells were cultured for 48 hr followed by staining of the membrane with a Diff-Quik stain kit. The number of cells that penetrated the membrane was counted in five microscopic fields (at 200× magnification) per filter. Invasive ability was defined as the proportion of cells that invaded the matrix-coated membrane divided by the number of cells that migrated through the uncoated membrane (baseline migration). The results are reported as the mean of duplicate assays. *$P < 0.05$ for 100 ng/ml RANKL versus control and OPG treated samples.

control). RANKL induced invasion occurred in a dose-dependent manner (data not shown). Invasion of PC3 cells through collagen was blocked by the addition of OPG, indicating that RANKL activation of RANK is sufficient to lead to invasion (Fig. 6, $P < 0.05$ RANKL treated vs. OPG treated). This data demonstrates that RANKL stimulated invasion of PC3 cells in vitro and supports the hypothesis that RANKL may serve as a chemoattractant factor for RANK-expressing tumor cells in vivo.

DISCUSSION

A universal attribute that distinguishes cancer cells that have a high propensity to metastasize to the bone is their ability to initiate or accelerate bone remodeling. There is considerable experimental evidence that the co-opted bone microenvironment provides reciprocal feedback to support tumor growth and occurs in both osteolytic and osteoblastic bone metastases (reviewed in Ref. [15]).

In this study, we observed that PC3 prostate tumor co-opt the critical processes that govern osteoclastogenesis. We observed that interaction of PC3 cells with the bone microenvironment results in excessive RANKL levels within the bone stroma and an increased ratio of RANKL to OPG at local and systemic levels. The operative role of RANKL in PC3 tumor-induced osteoclastogenesis and bone lesions was proven by blocking RANKL in vivo with OPG-Fc which eliminated tumor-induced osteoclastogenesis and reduced skeletal lesions. Importantly, we also demonstrate that RANK is expressed in prostate tumor cell lines derived from different metastatic sites and from both androgen-dependent and androgen-independent tumors. RANKL can directly activate RANK on tumor cells as was shown by the stimulation of several biochemical signaling pathways in PC3 cells. Moreover, we demonstrate that RANKL stimulation alters the expression of genes involved in chemotaxis, migration, and invasion of cancer cells. These effects at 24 hr may reflect the direct activation of RANK or be a consequence of a cascade of downstream factors initiated by RANKL stimulation. The data suggest that RANKL may stimulate tumor cell metastases. This hypothesis is supported by our observation that RANKL can activate the invasive/metastatic behavior of PC3 cells in vitro.

The critical involvement of RANKL in bone lesion formation and progression of prostate tumor growth within the skeleton has been well established in animal models of prostate cancer bone metastasis. Pharmacological inhibition of RANKL using recombinant constructs of either OPG-Fc or RANK-Fc in these models reduces tumor induced osteoclast numbers [18,36–38]. The reduction in osteoclastic activity presumably also blocks the release of growth factors [e.g., including transforming growth factor β (TGF-β), fibroblast growth factors (FGFs), platelet-derived growth factors (PDGFs), bone morphogenic proteins (BMPs), and insulin-like growth factor (IGF-1)] from the bone which normally would stimulate tumor growth. Thus, one mechanism by which RANKL inhibition reduces skeletal tumor burden is indirect, via inhibition of osteoclast activity and reduction of bone-derived growth factors [37–39]. The dependency of this effect on the bone microenvironment is supported by the observation that RANKL inhibition with OPG-Fc or RANK-Fc does not reduce the tumor growth of subcutaneously implanted prostate cancer cells [21,37,38].

While RANK expression has been primarily observed on osteoclasts, recent studies have demonstrated RANK expression on tumor cells, including breast, prostate, and melanoma cancer cell lines [19,20,26,40,41]. The ability of RANKL to act directly on RANK-expressing tumor cells that we observe in this study is consistent with a recently described role for RANKL in migration of prostate tumor cells [20] or other tumor cells [19]. Given the stimulation of tumor cell migration by RANKL, the authors of this study suggest that the rich source of RANKL within the bone may serve as a soil factor which attracts RANK-expressing tumor cells. To test this hypothesis, Jones et al., inhibited RANKL in a bone metastasis model in which the RANK-expressing melanoma does not lead to osteoclastic activation. The observed decrease in tumor growth in long bones with RANKL inhibition (using OPG-Fc) but not bisphosphonates, which suppress osteoclast activation, suggests that RANKL may act directly on tumor cells presumably via activation of cell migration [19].

In our own study we observed that RANKL inhibition with OPG-Fc reduced not only tumor-induced osteoclastogenesis and osteolytic lesions but also reduced PC3 skeletal tumor burden in a setting in which skeletal tumor and lesions were already established prior to treatment. Based on our observations of direct activation of RANK-expressing tumor cells by RANKL and the increased stromal levels of RANKL observed after PC3 interaction with the bone, there is potential for OPG-Fc to have a direct inhibitory effect on tumor cells. However, it is difficult to distinguish between direct and indirect effects of RANKL inhibition in vivo because of the degree of osteolysis induced by the tumor cells. One way in which OPG-Fc probably acts to reduce PC3 skeletal tumor burden is via indirect action on the bone microenvironment and interruption of the skeletal support of tumor growth. The identification in this current study of specific molecular markers of RANKL response in the PC3 cells (e.g.,

biochemical pathways, mRNA) will facilitate the development of pharmacodynamic markers of RANKL inhibition that can be used to demonstrate a direct effect of RANKL inhibition on the tumor cell. These experiments are currently underway.

Prostate tumors will give rise to a heterogeneous mix of blastic and lytic bone lesions in patients suggesting the activation of both osteoblast and osteoclasts. However, analysis of the critical osteoclastic regulatory proteins, RANKL and OPG, has not shown a correlation between expression and severity of bone disease. For instance, serum OPG is increased in patients with bone metastases relative to patients with non-osseous metastases and primary tumors [42–45]. Given that the majority of prostate cancer patients with bone metastasis have elevated bone remodeling [7,8] the increase in OPG may be a compensatory response to skeletal remodeling or a consequence of the increased tumor burden. In patients with prostate cancer bone metastases, there is considerable evidence of tumor-induced osteoclastogenesis [7,8], however whether the main source of RANKL is from the tumor itself or the bone stroma is somewhat controversial. There are now three studies of clinical prostate bone metastasis using immunohistochemical staining for RANKL and OPG that have revealed expression in prostate tumor cells, but not the bone stroma surrounding the tumor [26,46,47]. In our own observations in this animal model of prostate cancer-induced lesions we clearly demonstrate an excessive RANKL/OPG ratio that can be observed at the local and systemic level. Through the use of species-specific PCR primers and antibodies, we show that the host contributes to the majority of RANKL and OPG changes, including a significant increase in stromal RANKL levels, while the tumor cell production of these factors is not significantly altered at the end of study (day 21). We report an increase in the mouse RANKL/OPG ratio, which is consistent with data from other observations in which osteolysis is present in disease settings [48]. The discrepancy between these clinical data [26,46,47] and our own presented here may be due in part to the PC3 model representing an extreme osteolytic response to prostate cancer while in patients there is a greater contribution of osteoblastic lesions. Alternatively, the poor sensitivity and technical challenges of immunohistochemical analysis of RANKL expression in decalcified clinical bone sections that provide obstacles to specific RANKL detection are not problematic in the PC3 bone metastases model. In fact these earlier findings of RANKL-positive prostate cancer cells within bone metastases have not been confirmed and more recent studies in clinical samples indicate that RANKL protein is elevated in the bone stroma [49]. It is formally possible that the PC3 cells did express RANKL at an earlier point prior to day 21 that was not addressed in our own study. Either human or mouse RANKL (or both) must be operating at an early point to cause osteolysis, since the RANKL inhibitor OPG-Fc blocked the progression of PC3-induced x-ray lesions from days 7 to 14 (Fig. 1A). Irrespective of the source of RANKL, RANKL inhibitors should reduce the tumor-induced osteoclastogenesis, as was clearly demonstrated in the current study.

Altogether, these data underscore the functional importance of a dysregulated RANK/RANKL/OPG axis in the pathophysiology of prostate cancer bone metastasis. Moreover, these data substantiate the newly established direct role for RANKL in the metastatic/invasive activity of tumor cells and support further studies in vivo on the role of RANKL and RANK in bone metastases.

ACKNOWLEDGMENTS

The authors would like to thank Michelle Chaisson for thoughtful scientific discussion and Holly Zoog for editorial assistance. This work was supported in part by National Cancer Institute Grants P01 CA093900 and SPORE 1 P50 CA69568.

REFERENCES

1. Carlin BI, Andriole GL. The natural history, skeletal complications, and management of bone metastases in patients with prostate carcinoma. Cancer 2000;88 (12 Suppl):2989–2994.
2. Coleman RE. Metastatic bone disease: Clinical features, pathophysiology and treatment strategies. Cancer Treat Rev 2001; 27(3):165–176.
3. Charhon SA, Chapuy MC, Delvin EE, Valentin-Opran A, Edouard CM, Meunier PJ. Histomorphometric analysis of sclerotic bone metastases from prostatic carcinoma special reference to osteomalacia. Cancer 1983;51(5):918–924.
4. Stewart AF, Vignery A, Silverglate A, Ravin ND, LiVolsi V, Broadus AE, Baron R. Quantitative bone histomorphometry in humoral hypercalcemia of malignancy: Uncoupling of bone cell activity. J Clin Endocrinol Metab 1982;55(2):219–227.
5. Urwin GH, Percival RC, Harris S, Beneton MN, Williams JL, Kanis JA. Generalised increase in bone resorption in carcinoma of the prostate. Br J Urol 1985;57(6):721–723.
6. Chaisson ML, Branstetter DG, Derry JM, Armstrong AP, Tometsko ME, Takeda K, Akira S, Dougall WC. Osteoclast differentiation is impaired in the absence of inhibitor of kappa B kinase alpha. J Biol Chem 2004;279(52):54841–54848.
7. Clarke NW, McClure J, George NJ. Morphometric evidence for bone resorption and replacement in prostate cancer. Br J Urol 1991;68(1):74–80.
8. Demers LM, Costa L, Lipton A. Biochemical markers and skeletal metastases. Cancer 2000;88 (12 Suppl):2919–2926.
9. Lacey D. RANK/RANKL/OPG biology. J Musculoskel Neuron Interact 2004;4(3):241–242.
10. Kong YY, Yoshida H, Sarosi I, Tan HL, Timms E, Capparelli C, Morony S, Oliveira-dos-Santos AJ, Van G, Itie A, Khoo W, Wakeham A, Dunstan CR, Lacey DL, Mak TW, Boyle WJ,

Penninger JM. OPGL is a key regulator of osteoclastogenesis, lymphocyte development and lymph-node organogenesis. Nature 1999;397(6717):315–323.

11. Lacey DL, Tan HL, Lu J, Kaufman S, Van G, Qiu W, Rattan A, Scully S, Fletcher F, Juan T, Kelley M, Burgess TL, Boyle WJ, Polverino AJ. Osteoprotegerin ligand modulates murine osteoclast survival in vitro and in vivo. Am J Pathol 2000;157(2):435–448.
12. Dougall WC, Glaccum M, Charrier K, Rohrbach K, Brasel K, De Smedt T, Daro E, Smith J, Tometsko ME, Maliszewski CR, Armstrong A, Shen V, Bain S, Cosman D, Anderson D, Morrissey PJ, Peschon JJ, Schuh J. RANK is essential for osteoclast and lymph node development. Genes Dev 1999;13(18):2412–2424.
13. Li J, Sarosi I, Yan XQ, Morony S, Capparelli C, Tan HL, McCabe S, Elliott R, Scully S, Van G, Kaufman S, Juan SC, Sun Y, Tarpley J, Martin L, Christensen K, McCabe J, Kostenuik P, Hsu H, Fletcher F, Dunstan CR, Lacey DL, Boyle WJ. RANK is the intrinsic hematopoietic cell surface receptor that controls osteoclastogenesis and regulation of bone mass and calcium metabolism. Proc Natl Acad Sci USA 2000;97(4):1566–1571.
14. Matsuzaki K, Udagawa N, Takahashi N, Yamaguchi K, Yasuda H, Shima N, Morinaga T, Toyama Y, Yabe Y, Higashio K, Suda T. Osteoclast differentiation factor (ODF) induces osteoclast-like cell formation in human peripheral blood mononuclear cell cultures. Biochem Biophys Res Commun 1998;246(1):199–204.
15. Roodman GD. Mechanisms of bone metastasis. N Engl J Med 2004;350(16):1655–1664.
16. Morony S, Capparelli C, Sarosi I, Lacey DL, Dunstan CR, Kostenuik PJ. Osteoprotegerin inhibits osteolysis and decreases skeletal tumor burden in syngeneic and nude mouse models of experimental bone metastasis. Cancer Res 2001;61(11):4432–4436.
17. Morony S, Capparelli C, Kostenuik P, Rattan A, Scully S, Tarpley J, Wiemann B, Starnes C, Lacey DL, Dunstan CR. Osteoprotegerin prevents bone destruction in athymic and syngeneic models of experimental tumor metastasis to bone. Cancer 2000;88(12):3107.
18. Zhang J, Dai J, Qi Y, Lin DL, Smith P, Strayhorn C, Mizokami A, Fu Z, Westman J, Keller ET. Osteoprotegerin inhibits prostate cancer-induced osteoclastogenesis and prevents prostate tumor growth in the bone. J Clin Invest 2001;107(10):1235–1244.
19. Jones DH, Nakashima T, Sanchez OH, Kozieradzki I, Komarova SV, Sarosi I, Morony S, Rubin E, Sarao R, Hojilla CV, Komnenovic V, Kong YY, Schreiber M, Dixon SJ, Sims SM, Khokha R, Wada T, Penninger JM. Regulation of cancer cell migration and bone metastasis by RANKL. Nature 2006;440(7084):692–696.
20. Mori K, Le Goff B, Charrier C, Battaglia S, Heymann D, Redini F. DU145 human prostate cancer cells express functional receptor activator of NFkappaB: New insights in the prostate cancer bone metastasis process. Bone 2007;40(4):981–990.
21. Zhang J, Lu Y, Dai J, Yao Z, Kitazawa R, Kitazawa S, Zhao X, Hall DE, Pienta KJ, Keller ET. In vivo real-time imaging of TGF-beta-induced transcriptional activation of the RANK ligand gene promoter in intraosseous prostate cancer. Prostate 2004;59(4):360–369.
22. Fu Z, Smith PC, Zhang L, Rubin MA, Dunn RL, Yao Z, Keller ET. Effects of raf kinase inhibitor protein expression on suppression of prostate cancer metastasis. J Natl Cancer Inst 2003;95(12):878–889.
23. Corey E, Quinn JE, Bladou F, Brown LG, Roudier MP, Brown JM, Buhler KR, Vessella RL. Establishment and characterization of osseous prostate cancer models: Intra-tibial injection of human prostate cancer cells. Prostate 2002;52(1):20–33.
24. Kalikin LM, Schneider A, Thakur MA, Fridman Y, Griffin LB, Dunn RL, Rosol TJ, Shah RB, Rehemtulla A, McCauley LK, Pienta KJ. In vivo visualization of metastatic prostate cancer and quantitation of disease progression in immunocompromised mice. Cancer Biol Ther 2003;2(6):656–660.
25. Fata JE, Kong YY, Li J, Sasaki T, Irie-Sasaki J, Moorehead RA, Elliott R, Scully S, Voura EB, Lacey DL, Boyle WJ, Khokha R, Penninger JM. The osteoclast differentiation factor osteoprotegerin-ligand is essential for mammary gland development. Cell 2000;103(1):41–50.
26. Chen G, Sircar K, Aprikian A, Potti A, Goltzman D, Rabbani SA. Expression of RANKL/RANK/OPG in primary and metastatic human prostate cancer as markers of disease stage and functional regulation. Cancer 2006;107(2):289–298.
27. Sramkoski RM, Pretlow TG II, Giaconia JM, Pretlow TP, Schwartz S, Sy MS, Marengo SR, Rhim JS, Zhang D, Jacobberger JW. A new human prostate carcinoma cell line, 22Rv1. In Vitro Cell Dev Biol Anim 1999;35(7):403–409.
28. Thalmann GN, Anezinis PE, Chang SM, Zhau HE, Kim EE, Hopwood VL, Pathak S, von Eschenbach AC, Chung LW. Androgen-independent cancer progression and bone metastasis in the LNCaP model of human prostate cancer. Cancer Res 1994;54(10):2577–2581.
29. Anderson DM, Maraskovsky E, Billingsley WL, Dougall WC, Tometsko ME, Roux ER, Teepe MC, DuBose RF, Cosman D, Galibert L. A homologue of the TNF receptor and its ligand enhance T-cell growth and dendritic-cell function. Nature 1997;390(6656):175–179.
30. Galibert L, Tometsko ME, Anderson DM, Cosman D, Dougall WC. The involvement of multiple tumor necrosis factor receptor (TNFR)-associated factors in the signaling mechanisms of receptor activator of NF-kappaB, a member of the TNFR superfamily. J Biol Chem 1998;273(51):34120–34127.
31. Wong BR, Besser D, Kim N, Arron JR, Vologodskaia M, Hanafusa H, Choi Y. TRANCE, a TNF family member, activates Akt/PKB through a signaling complex involving TRAF6 and c-Src. Mol Cell 1999;4(6):1041–1049.
32. Reiland J, Furcht LT, McCarthy JB. CXC-chemokines stimulate invasion and chemotaxis in prostate carcinoma cells through the CXCR2 receptor. Prostate 1999;41(2):78–88.
33. Geiser T, Dewald B, Ehrengruber MU, Clark-Lewis I, Baggiolini M. The interleukin-8-related chemotactic cytokines GRO alpha, GRO beta, and GRO gamma activate human neutrophil and basophil leukocytes. J Biol Chem 1993;268(21):15419–15424.
34. Breuil V, Schmid-Antomarchi H, Schmid-Alliana A, Rezzonico R, Euller-Ziegler L, Rossi B. The receptor activator of nuclear factor (NF)-kappaB ligand (RANKL) is a new chemotactic factor for human monocytes. FASEB J 2003;17(12):1751–1753.
35. Henriksen K, Karsdal M, Delaisse JM, Engsig MT. RANKL and, vascular endothelial growth factor (VEGF) induce osteoclast chemotaxis through an ERK1/2-dependent mechanism. J Biol Chem 2003;278(49):48745–48753.
36. Whang PG, Schwarz EM, Gamradt SC, Dougall WC, Lieberman JR. The effects of RANK blockade and osteoclast depletion in a model of pure osteoblastic prostate cancer metastasis in bone. J Orthop Res 2005;23(6):1475–1483.
37. Zhang J, Dai J, Yao Z, Lu Y, Dougall W, Keller ET. Soluble receptor activator of nuclear factor kappaB Fc diminishes prostate cancer progression in bone. Cancer Res 2003;63(22):7883–7890.

38. Yonou H, Kanomata N, Goya M, Kamijo T, Yokose T, Hasebe T, Nagai K, Hatano T, Ogawa Y, Ochiai A. Osteoprotegerin/osteoclastogenesis inhibitory factor decreases human prostate cancer burden in human adult bone implanted into nonobese diabetic/severe combined immunodeficient mice. Cancer Res 2003;63(9):2096–2102.
39. Kiefer JA, Vessella RL, Quinn JE, Odman AM, Zhang J, Keller ET, Kostenuik PJ, Dunstan CR, Corey E. The effect of osteoprotegerin administration on the intra-tibial growth of the osteoblastic LuCaP 23.1 prostate cancer xenograft. Clin Exp Metastasis 2004; 21(5):381–387.
40. Tometsko M, Armstrong A, Miller R, Jones J, Chaisson M, Branstetter D, Dougall W. RANK ligand directly induces osteoclastogenic, angiogenic, chemoattractive and invasive factors on RANK-expressing human cancer cells MDA-MB-231 and PC3. J Bone Miner Res 2004;19 (Suppl 1):S25, abstract #1095.
41. Thomas RJ, Guise TA, Yin JJ, Elliott J, Horwood NJ, Martin TJ, Gillespie MT. Breast cancer cells interact with osteoblasts to support osteoclast formation. Endocrinology 1999;140(10):4451–4458.
42. Jung K, Stephan C, Semjonow A, Lein M, Schnorr D, Loening SA. Serum osteoprotegerin and receptor activator of nuclear factor-kappa B ligand as indicators of disturbed osteoclastogenesis in patients with prostate cancer. J Urol 2003;170 (6 Pt 1):2302–2305.
43. Eaton CL, Wells JM, Holen I, Croucher PI, Hamdy FC. Serum osteoprotegerin (OPG) levels are associated with disease progression and response to androgen ablation in patients with prostate cancer. Prostate 2004;59(3):304–310.
44. Brown JM, Vessella RL, Kostenuik PJ, Dunstan CR, Lange PH, Corey E. Serum osteoprotegerin levels are increased in patients with advanced prostate cancer. Clin Cancer Res 2001;7(10): 2977–2983.
45. Jung K, Lein M, Stephan C, Von Hosslin K, Semjonow A, Sinha P, Loening SA, Schnorr D. Comparison of 10 serum bone turnover markers in prostate carcinoma patients with bone metastatic spread: Diagnostic and prognostic implications. Int J Cancer 2004;111(5):783–791.
46. Brown JM, Corey E, Lee ZD, True LD, Yun TJ, Tondravi M, Vessella RL. Osteoprotegerin and rank ligand expression in prostate cancer. Urology 2001;57(4):611–616.
47. Perez-Martinez FC, Alonso V, Sarasa JL, Nam-Cha SG, Vela-Navarrete R, Manzarbeitia F, Calahorra FJ, Esbrit P. Immunohistochemical analysis of low-grade and high-grade prostate carcinoma: Relative changes of pthrp and its pth1 receptor, osteoprotegerin and receptor activator of nuclear factor-kb ligand. J Clin Pathol 2006.
48. Grimaud E, Soubigou L, Couillaud S, Coipeau P, Moreau A, Passuti N, Gouin F, Redini F, Heymann D. Receptor activator of nuclear factor kappaB ligand (RANKL)/osteoprotegerin (OPG) ratio is increased in severe osteolysis. Am J Pathol 2003;163(5): 2021–2031.
49. Roudier M, Morrissey C, Huang L-Y, Warren A, Rohrbach K, Koelling R, Keller E, Vessella R, Dougall WC. Differential Expression of RANK/RANKL/OPG in prostate cancer bone and soft tissue metastases. Cancer Treat Rev 2006;32 (Suppl 3): S13, abstract #10.